Research Article

Chemical Space Expansion of Bromodomain Ligands Guided by in Silico Virtual Couplings (AutoCouple)

Laurent Batiste,[†,‡] Andrea Unzue,[‡,§] Aymeric Dolbois,[§] Fabrice Hassler,[§] Xuan Wang,[†,§] Nicholas Deerain,[†] Jian Zhu,[†] Dimitrios Spiliotopoulos,[†] Cristina Nevado,*[,§] and Amedeo Caflisch*[,†]

[†]Department of Biochemistry, University of Zurich, Winterthurerstrasse 190, CH-8057, Zürich, Switzerland
[§]Department of Chemistry, University of Zurich, Winterthurerstrasse 190, CH-8057, Zürich, Switzerland

ⓢ Supporting Information

ABSTRACT: Expanding the chemical space and simultaneously ensuring synthetic accessibility is of upmost importance, not only for the discovery of effective binders for novel protein classes but, more importantly, for the development of compounds against hard-to-drug proteins. Here, we present AutoCouple, a de novo approach to computational ligand design focused on the diversity-oriented generation of chemical entities via virtual couplings. In a benchmark application, chemically diverse compounds with low-nanomolar potency for the CBP bromodomain and high selectivity against the BRD4(1) bromodomain were achieved by the synthesis of about 50 derivatives of the original fragment. The binding mode was confirmed by X-ray crystallography, target engagement in cells was demonstrated, and antiproliferative activity was showcased in three cancer cell lines. These results reveal AutoCouple as a useful in silico coupling method to expand the chemical space in hit optimization campaigns resulting in potent, selective, and cell permeable bromodomain ligands.
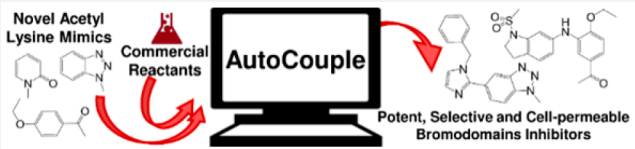
INTRODUCTION

The druglike chemical space is estimated at 10^{60} organic molecules, but only 100 million have been synthesized to date, and an even smaller fraction thereof is commercially available.[1,2] Libraries of purchasable molecules are biased toward certain classes of targets, in particular G-protein-coupled receptors and kinases.[3,4] Repositories of pharmaceutical companies consist of 10^6 to 10^7 compounds which barely scratch the surface of chemical space. Success in high-throughput screening ultimately relies on the screening library:[5−7] the exploration of chemical space that is not biased toward already investigated targets is decisive not only for the discovery of effective binders for novel protein classes but, more importantly, for the development of compounds against protein targets that are hard-to-drug.[8−11] Classical de novo strategies can potentially populate new areas of chemical space,[12−16] and thus, programs have been developed to disconnect molecules following retrosynthesis rules[17,18] producing fragments that can be used later on to construct new libraries.[19] Nevertheless, significant challenges when reaching the synthesis stage might prevent those new molecular entities from being prepared and, ultimately, becoming useful chemical probes.[13] In addition, time pressure in drug-discovery campaigns demands new tools to improve the identification of hits and streamline their optimization into lead compounds.[20] Computational tools for de novo generation of molecular entities via virtual couplings have been reported.[21−24] The method proposed here, called AutoCouple, distinguishes itself by starting from a set of available building blocks that are assembled via virtual organic reactions in such a way that, at the coupling step, the reaction partners are parsed automatically and are coupled only if no undesired group is contained (e.g., groups that would require additional protection steps or lead to cross reactivity products are discarded). As such, AutoCouple generates libraries of compounds that are, ideally, synthesizable in one step.

Bromodomains are protein modules that bind acetylated lysine (KAc) residues in histone tails and other proteins. Among the 61 known human bromodomains,[25] the BET family, in particular BRD4(1) (the first bromodomain of the protein called BRD4), has been widely targeted because of its involvement in cancer, type 2 diabetes, and cardiovascular diseases.[26−30] Several small molecule ligands of BET bromodomains are currently in clinical trials, which highlights the potential of regulating post-transcriptional modifications of histone tails in the current landscape of drug discovery.[31−34] In contrast, selective and potent bromodomain ligands, aiming to unravel the biological implications of bromodomains outside the BET family, have only recently started to be developed.[35−54] In particular, the bromodomain of CBP (the epigenetic reader of the cyclic AMP response element binding protein) is an interesting target due to its key role in several diseases including cancer and neurological disorders.[55] Despite recent efforts toward developing novel and selective CBP bromodomain inhibitors, the chemotypes that are able to act as KAc mimic are still rather limited and, except for GNE-781, demand exquisite absolute stereocontrol, thus complicating their synthetic accessibility (Figure 1A).[56−67]

Our groups have recently reported the fragment-based design[68,69] of acetyl benzene derivatives as selective nanomolar
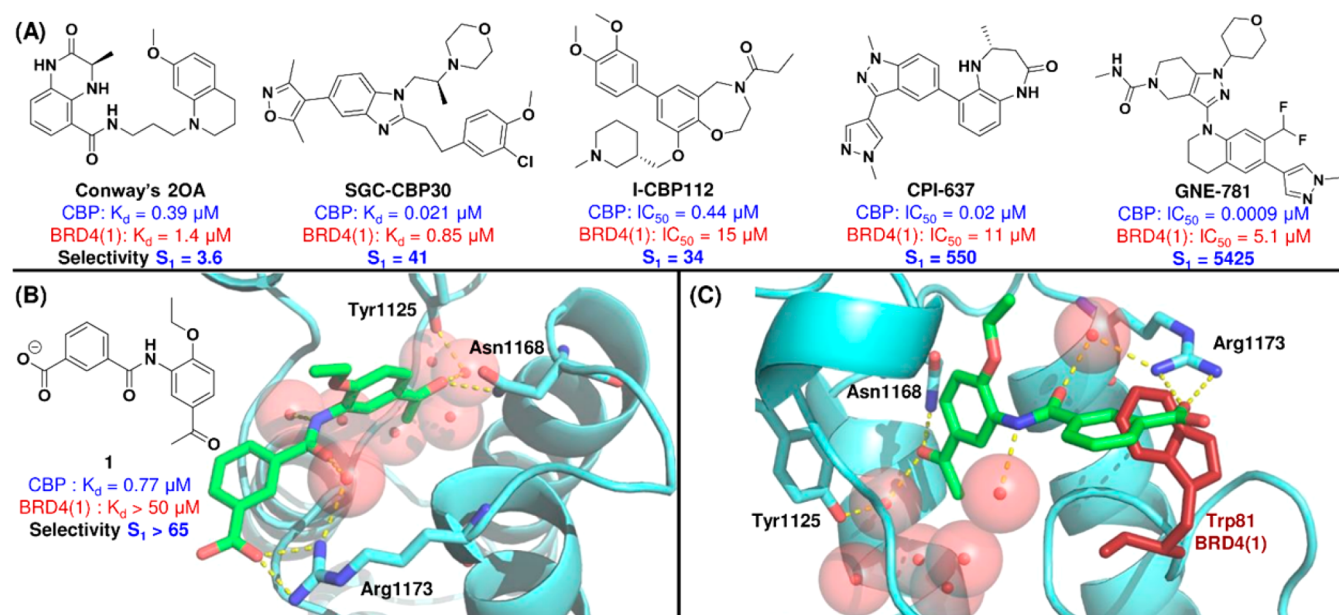
Figure 1. (A) List of current nM inhibitors of the CBP bromodomain.[44,56−58,60] Dissociation constant (K_d) determined by isothermal titration calorimetry (ITC). Half-maximal inhibitory concentration (IC_{50}) determined by time-resolved fluorescence resonance energy transfer (TR-FRET). Selectivity for CBP over BRD4(1) bromodomains (S_1) determined by the ratio of K_d or IC_{50} values. (B) Crystal structure of the CBP bromodomain (cyan) in complex with compound **1** (green) (PDB code: 4TQN).[70,71] The acetyl benzene moiety acts as a KAc mimic interacting directly and through a water molecule with the side chains of the conserved residues Asn1168 and Tyr1125, respectively. The carboxylate function of the tail group forms a salt bridge with the guanidinium of Arg1173. The amide linker is involved in two water-bridged hydrogen bonds with the CBP bromodomain. (C) Overlay of the complex of compound **1** (green) with the CBP bromodomain (cyan) and the structure of BRD4(1) (4PCI) shows that the selectivity is due to bumping of the benzoate into the Trp81 side chain (red) of the so-called WPF triad of BRD4(1).
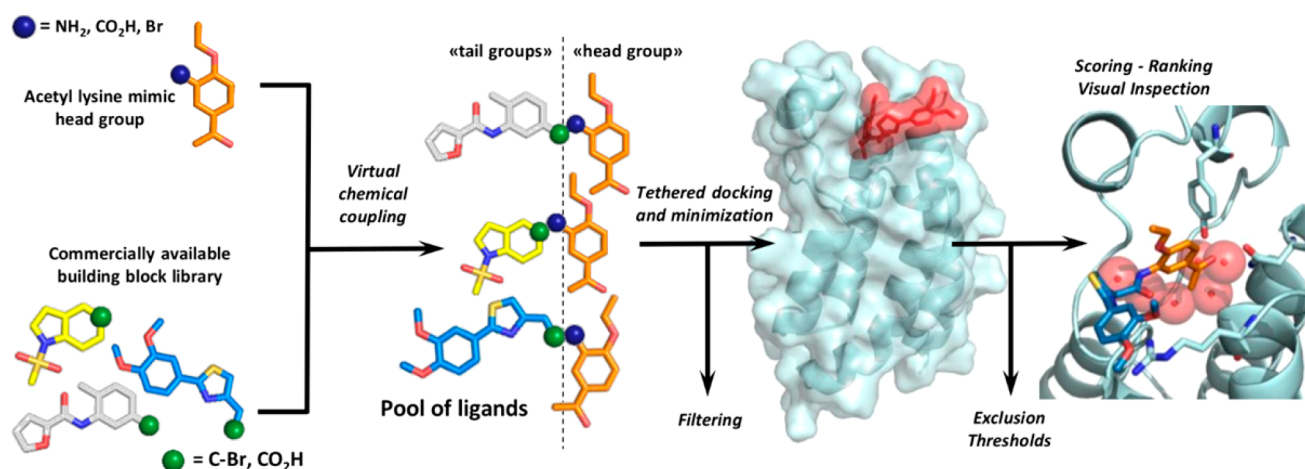

Figure 2. Schematic representation of AutoCouple. A headgroup (here the KAc mimic is shown in orange) is virtually coupled to commercially available building blocks. The resulting library is filtered out to remove any protein-reactive functionalities and subsequently docked while maintaining key interactions of the headgroup inside the target's binding site. The compounds are ranked according to binding energy calculated by a force field with continuum electrostatic solvation.

CBP bromodomain ligands.[70,71] Compound **1** (Figure 1B), bearing a benzoic acid moiety, proved to be a synthetically accessible molecule with an equilibrium dissociation constant (K_d) of 770 nM for the CBP bromodomain and good selectivity over BRD4(1) (selectivity >65-fold according to the ratio of K_d values). The overlap of the crystal structures of the complex of compound **1** with the CBP bromodomain and the structure of BRD4(1) (Figure 1C) shows that the selectivity is due to the steric clash between the benzoate group and the Trp81 side chain of the so-called WPF triad of BRD4(1). Further development of this compound was not pursued given its lack of target engagement in cells, likely due to the negative

effect of the carboxylate on the compound's permeability, a commonly encountered problem in medicinal chemistry optimization campaigns.[72−74] We thus set out to identify new chemotypes enabling interactions at the outer part of the binding site of the CBP bromodomain (Arg1173 and/or the so-called ZA loop) that could potentially translate into ligands with improved potency, selectivity, and cell permeability compared to hit **1**.

To this end, we sought to establish an efficient method for growing fragments into potent and selective ligands taking chemical accessibility into account at the outset of the computation.[75,76] This early on synthesis oriented approach

Scheme 1. AutoCouple Results for the CBP Bromodomain Using (A) Amide Condensation, (B) Buchwald–Hartwig Amination, and (C) Suzuki Cross-Coupling Reactions from Aniline (2), Bromobenzene (3), and Aryl Boronic Ester (4) as "Headgroups", Respectively[a]
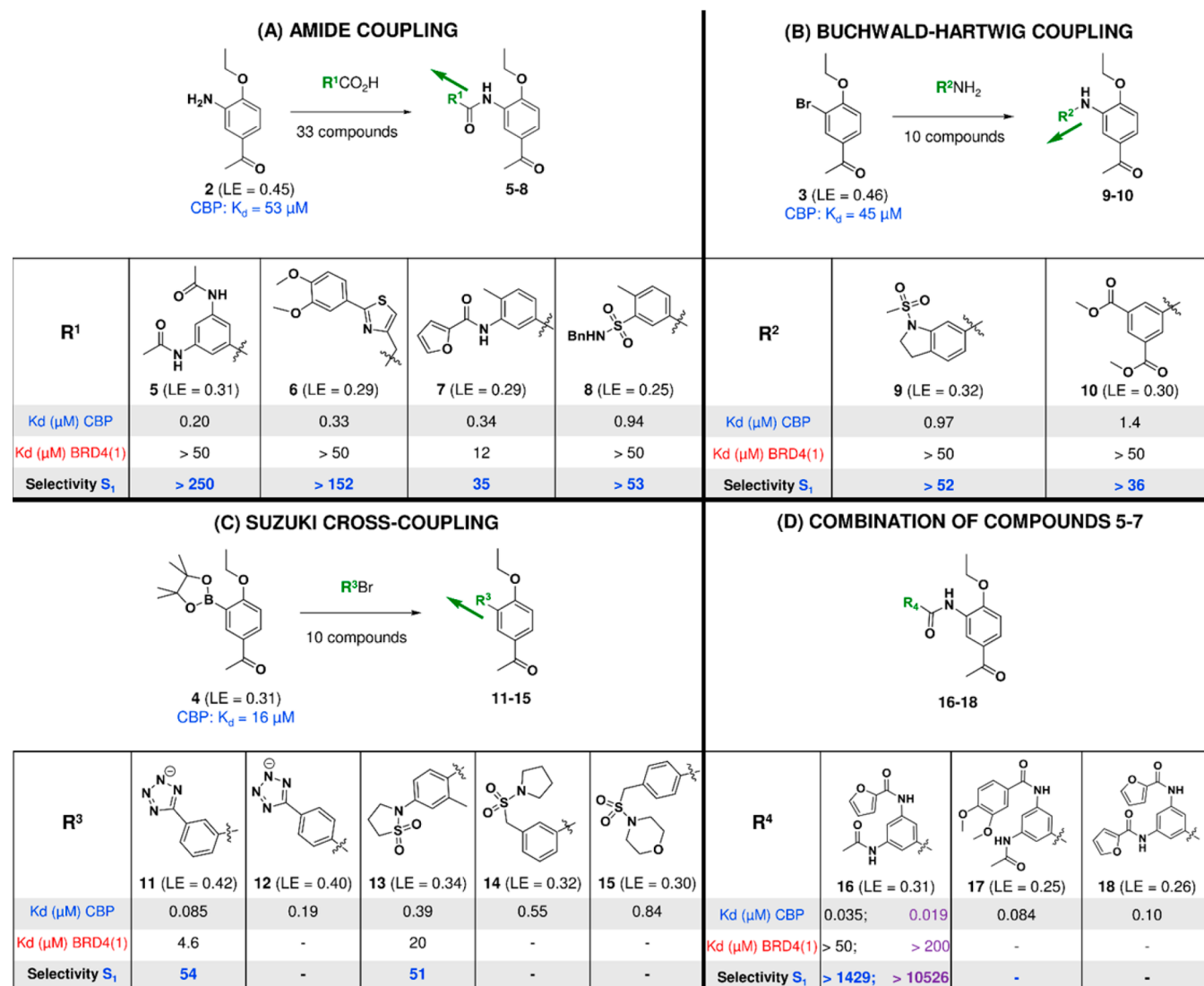
[a] K_d values (μM) were determined by a competition binding assay in duplicates (BROMOscan).[88] IC$_{50}$ values for compound 16 are indicated in purple and were determined by amplified luminescent proximity homogeneous assay (Alpha) screen technology (Reaction Biology). Ligand efficiency (LE) values refer to the CBP bromodomain. Selectivity for CBP over BRD4(1) bromodomains (S_1) determined by the ratio of K_d or IC$_{50}$ values. (D) Chimerization of compounds 5–7. The growing vectors (green arrows) of the different coupling strategies show the similarity between the amide and the C–C coupled products compared to the amine linker in orienting the tail group.

would confer on our method the possibility to overcome the limitations of previously released software tools which typically suggest hard-to-synthesize molecules, hampering follow-up medicinal chemistry efforts. Here, we present the realization of this concept with AutoCouple, a novel approach to de novo computational ligand design that focuses on the diversity-oriented generation of chemical entities via virtual chemical couplings. AutoCouple is the first fragment-growing software tool that generates synthetically accessible molecules with a force field based prediction of their binding energy without any fitting parameter. Its operative and pragmatic value has been demonstrated by the discovery of novel chemical blueprints which translated into nM potent and cell-permeable inhibitors of the CBP bromodomain with high selectivity over BRD4(1). Further, the preliminary biological evaluation of cell permeable

ligands points toward the potential use of these compounds to unravel the role of CBP in several types of solid tumors and hematological malignancies.[77]

■ RESULTS AND DISCUSSION

Implementation of AutoCouple and Application to CBP Bromodomain. First, a suite of Python scripts[78,79] was assembled (see section 1 in the Supporting Information) to generate a virtual library from commercially available reagents by a set of coupling reactions suited for medicinal chemistry (Figure 2). Three reactions were established based on the following criteria:[5,80] (a) the robustness of the intended chemical coupling, (b) the applicability to a wide variety of reactants, (c) the proven relevance/use in drug-discovery campaigns. The acetyl benzene moiety within 1 was retained as
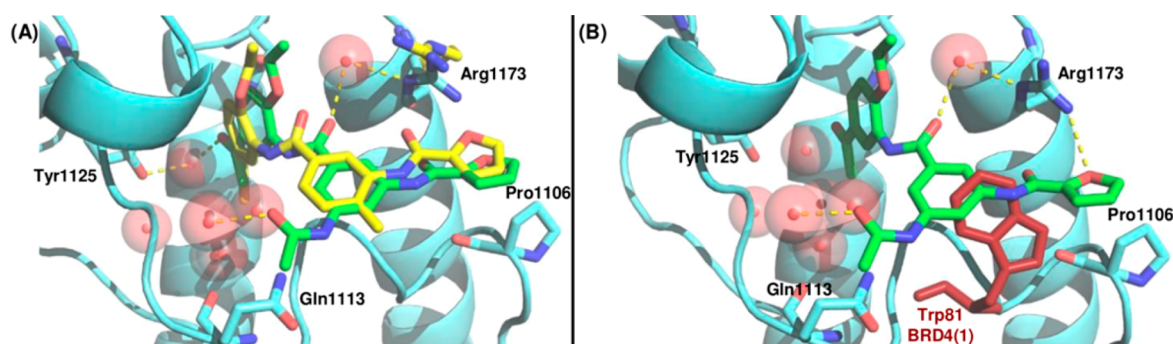
Figure 3. (A) Structural alignment of the crystal structure of the CBP bromodomain (cyan) in complex with ligand **16** (green) (PDB code 5NLK) and the pose of ligand **7** (yellow) as predicted by docking into the CBP structure 4NYX (Arg1173 side chain in yellow). (B) Overlay of the complex of compound **16** (green) with the CBP bromodomain (cyan) and the structure of BRD4(1) (4PCI) shows that the selectivity is due to bumping of the phenyl into the Trp81 side chain (red) of the so-called WPF triad of BRD4(1).

the KAc mimic (from now on referred to as "headgroup"), and we thus decided to explore the chemical space of the "tail group" adjacent to the KAc mimic.

First, commercially available building block libraries were generated, followed by coupling in silico to the KAc mimic in compound **1**. Aniline **2**, bromobenzene **3**, and aryl boronic ester **4** were selected as "headgroups" for amide condensation, Buchwald−Hartwig amination, and Suzuki cross-coupling, respectively (Schemes 1A, 1B, and 1C respectively). For the tail, a library of ~270,000 commercially available compounds was sorted according to chemical functionalities. A series of filters were applied to limit the final molecular complexity and to discard molecular patterns known to react non-specifically with most proteins[81,82] as well as heavy metals containing molecules. Moreover, to avoid redundancies, any building blocks with the same CAS number were merged. Considering that chemical couplings imply an increase in the molecular complexity (except for cleavage reactions),[22] and that the coupling products should preferably satisfy the Lipinski rule of 5 for druglikeness, building blocks meeting any of the following criteria were discarded: (a) >5 rotatable bonds; (b) number of heavy atoms (= non-hydrogen) smaller than 3 or larger than 35; (c) >2 chiral centers. Each virtual reaction was also encoded to discard any building block that contained undesired chemical functionalities that would require a protecting group or lead to cross-reactivity problems. For instance, for the Buchwald−Hartwig coupling, the amine building blocks containing a halide (which would ultimately lead to self-condensation) were not kept for the virtual reactions.

A total of ~70,000 virtual compounds were generated: 32,000 carboxylic amides (A), 19,000 anilines (B), and 19,000 C−C coupled ligands (C). Five independent docking campaigns were carried out with libraries A, B, and C using the CBP bromodomain structures 3P1C, 4TQN, and 4NYX (see section 1.3 in the Supporting Information). Multiple crystal structures were used because of the flexibility of the Arg1173 side chain and the rigid-protein protocol employed for docking by the open-source software rDock.[83] The acetyl benzene was initially oriented in the binding site to mimic the KAc residue as observed in the crystal structure and then underwent flexible docking. The poses obtained by docking were subsequently minimized using the CHARMM program[84] and the CHARMM36/CGenFF force field[85,86] with evaluation of desolvation effects in the continuum dielectric approximation.[87] Receiver operating characteristic (ROC) curves using known positive controls[70,71] were plotted as to ensure the

ability of the force field and implicit solvent approximation (finite-difference Poisson) to prioritize active ligands.

Synthesis of de Novo Ligand Binders: Potency, Selectivity, and Binding Mode Validation. Overall, 53 top-ranking compounds were synthesized (Scheme 1A−C) and a competition binding assay (BROMOscan)[88] was used to measure dissociation constants (for exhaustive data on all synthesized ligands, see section 2 in the Supporting Information). Using amide coupling for fragment assembly enabled us to identify arylsulfonamides, -acetamides, and -thiazoles with diverse substitution patterns (**5−8**) as suitable motifs to replace the original benzoate "tail group". These de novo synthesized ligands displayed comparable or even improved levels of potency and selectivity compared to those previously observed for **1**. Compound **5** showed not only a 4-fold improvement in potency (K_d = 200 nM) but also a remarkably high selectivity (>250-fold) against BRD4(1). Furthermore, the "amide-coupling" campaign resulted in 33 synthesized molecules, four of which display submicromolar affinity (compounds **5−8**, Scheme 1A), 17 are low micromolar binders (1.2−6.5 μM), and 10 have K_d values between 10 μM and 45 μM (see Figure S1). Compounds stemming from both Buchwald−Hartwig amination (**9**, **10**) and Suzuki cross-coupling (**11−15**) consistently showed improved affinities and good selectivity while offering additional motifs (cyclic and linear alkylsulfonamides, diester, tetrazoles) to the portfolio of "tail groups" for CBP ligands (Scheme 1B,C).

Interestingly, five out of 10 molecules synthesized by Suzuki cross-couplings are nanomolar binders with K_d values ranging from 85 to 840 nM (Scheme 1C, compounds **11−15**), thus confirming the ability of AutoCouple to identify good binders.

The comparison between the three series of compounds (A, B, C) confirms that the amide linker does not contribute significantly to binding affinity, which is consistent with previous molecular dynamics simulations that showed rotations of the amide group on the 100 ns time scale.[70,89] In addition, the analysis of the growing vectors of the three coupling strategies reveals interesting trends. As shown by the green arrows (growing vectors) in Scheme 1, a geometric similarity between the amide and the C−C coupled products (A, C) can be found, in line with the consistently higher potency observed for the compounds obtained via these two reactions compared to those introducing the amine linker (B).

The preparation of an analogue of compound **1** bearing a triazole as KAc mimic (Table S2) turned out to be more selective for BRD4(1) over CBP, suggesting that the selectivity
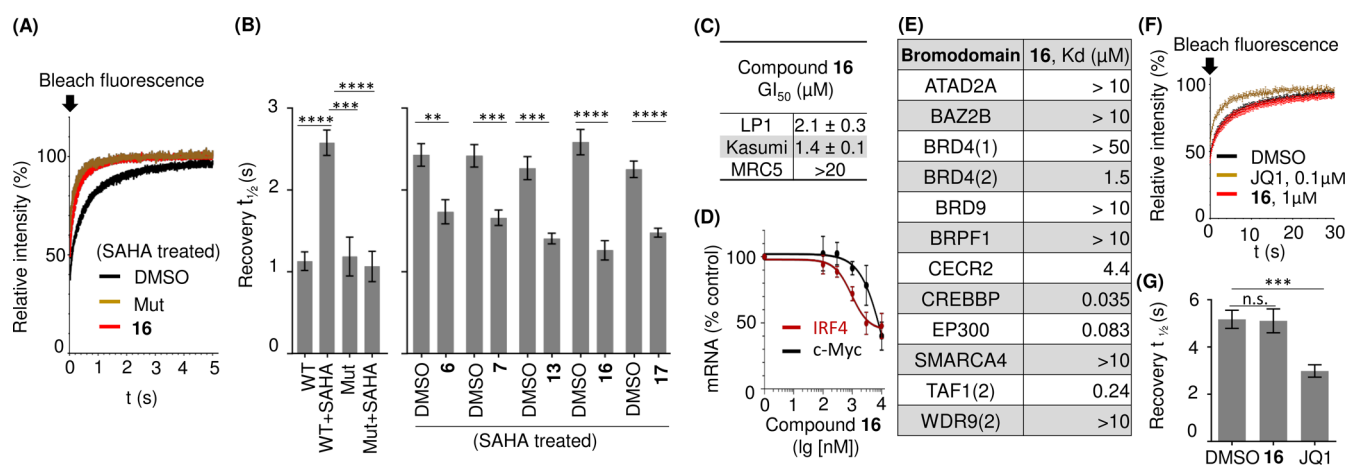
Figure 4. (A,B) FRAP assay for compounds **6**, **7**, **13**, **16**, and **17**; U2OS cells were transfected with plasmids encoding GFP-fused to wild-type (WT) or mutant (N1168F) multimerized CBP bromodomain, with or without 2.5 μM suberoylanilide hydroxamic acid (SAHA, a deacetylase inhibitor) and indicated compounds at a concentration of 1 μM. (A) Fluorescent recovery curves after photobleaching (normalized to the intensity before bleaching). (B) Half-times of the fluorescence recovery ($t_{1/2}$) ($n \geq 7$ cells per group, error bars: standard error of the mean). The recovery $t_{1/2}$ of the compound-treated cells was compared to that of DMSO-treated cells (bar on the left) within the same experiment setup using Mann−Whitney test. **, $P < 0.01$; ***, $P < 0.001$; ****, $P < 0.0001$. (C) Concentration of compound **16** that results in 50% growth inhibition (GI50). LP1 and Kasumi are human tumor cell lines while the nontransformed fibroblast MRC5 is a negative control. GI50 values were determined by a resazurin assay after 72 h compound incubation. (D) Dose-dependent inhibition of IRF4 and c-Myc mRNA transcription (RT-qPCR) by compound **16** in LP1 cells after 6 h of treatment. (C, D) Values represent the mean of at least three biological replicates $\pm$ SD. The curves are fits by a four-parameter logistic function. (E) Selectivity profile of compound **16** in a panel of bromodomains representing all subfamilies of human bromodomains. The K_d values were determined by a competition binding assay.[88] (F, G) FRAP assay for compound **16** in U2OS cells transfected with a plasmid encoding GFP-BRD4. Cells were treated with compound **16** (1 μM) or a BRD4 ligand JQ1 (0.1 μM). (F) Fluorescent recovery curves after photobleaching (normalized to the intensity before bleaching). (G) $t_{1/2}$ in the FRAP assay of F ($n \geq 7$ cells per group, error bars: standard error of the mean, Mann−Whitney test; ***, $P < 0.001$; n.s., not significant).

can possibly arise from the KAc mimic moiety.[90] AutoCouple was therefore further validated through a virtual-coupling campaign to design BRD4(1) inhibitors (detailed information is available in section 3 in the Supporting Information).

Hybridization Strategies. Aiming to further improve the affinity of these compounds, we decided to combine the best performing motifs in the amide-coupling campaign (acetamide **5**, dimethoxybenzene **6**, and furan **7**) into compounds **16−18**. This hybridization approach resulted in additional low nanomolar CBP ligands (Scheme 1D). Remarkably, compound **16** shows an affinity for the CBP bromodomain higher by a factor of more than 10,000 with respect to the affinity for the BRD4(1) bromodomain while still exhibiting an excellent ligand efficiency for the target of 0.31 and 0.32 kcal mol^{-1} per non-hydrogen atom (according to BROMOscan and AlphaScreen, respectively) in line with recommendations for maintaining druglike properties throughout the optimization process.[91,92]

The crystal structure of CBP in complex with ligand **16** (PDB code 5NLK) could be obtained, confirming that the binding mode predicted by AutoCouple is correct (Figure 3A): the furan ring of compound **16** is at favorable van der Waals distance to the Pro1106 side chain as predicted by the docked pose of the parent compound **7**. The overlap of the crystal structure of the CBP/ligand **16** complex with the BRD4(1) structure shows steric conflicts with the Trp81 side chain (Figure 3B), which explains its high selectivity.[59,60] Compound **16** was further profiled via a BROMOscan against a panel of bromodomains covering all subfamilies (Figure 4E). While the strong binding to CREBBP and EP300 could again be confirmed, only moderate affinity for the bromodomains of CECR2 (the bromodomain of the cat eye syndrome critical region protein 2) and TAF1(2) (the second bromodomain of

human transcription initiation factor TFIID subunit 2) was observed.[93]

Target Engagement in Cells and Preliminary Biological Evaluation. The target engagement of some of these ligands and thus their cell permeability were evaluated by means of a fluorescence recovery after photobleaching (FRAP) assay.[94] In human osteosarcoma U2OS cells, compounds **6**, **7**, **13**, **16**, and **17** at a concentration of 1 μM showed significant displacement of the GFP-fused CBP bromodomain from chromatin. In particular, compound **16**, which displayed the highest affinity for the CBP bromodomain in the biochemical assay ($K_d = 35$ nM), showed also the strongest effect in the FRAP assay (Figure 4A,B). The compounds' purity was evaluated by peak integration of the UV/visible HPLC chromatograms for compounds **6** (99%), **7** (94%), **13** (99%), **16** (97%), and **17** (92%) (see section 11 in the SI).

Compound **16** was further tested in cellular proliferation assays. Three cell lines known to be sensitive to CBP bromodomain inhibition, i.e., LP1 (multiple myeloma), Kasumi, and HL-60 (acute myeloblastic leukemia),[59,95] were selected as well as nontransformed primary fibroblast MRC5.[96] The MRC5 cells are used as control as they are noncancer cells and with limited lifespan caused by replicative senescence.[97] The resazurin assay was employed with compound incubation for 72 h (LP1, Kasumi, and MRC5; Figure 4C) or 144 h (LP1, Kasumi, and HL-60; Figure S9).[98] Remarkably, compound **16** selectively inhibited the proliferation of the three cancer cell lines, but was not toxic in MRC5 cells (GI50 > 20 μM) (Figure 4C, Figures S8 and S9). Since CBP and EP300 regulate the transcription of the lymphocyte-specific transcription factor IRF4 and the IRF4 target gene c-MYC in myeloma cells,[59,60] we investigated the transcription of IRF4 and c-MYC in the LP1 cell line using RT-qPCR (reverse transcription quantitative

polymerase chain reaction). The dose−response curves showed that the mRNA levels of IRF4 and c-MYC were reduced after incubation for 6 h with compound **16** (Figure 4D). Since the inhibition of BRD4 bromodomains also has a strong effect on c-MYC expression,[99] one could argue that the c-MYC inhibition by compound **16** arises from a weak binding to the BRD4 protein. To address this issue, we evaluated the BRD4 engagement in cells by FRAP. Compound **16** at 1 μM showed no effect on the fluorescence recovery time (Figure 4F,G), thus confirming the potential of compound **16** as a useful tool to unravel the specific role of CBP bromodomain in disease.

CONCLUSIONS

A de novo design approach based on virtual chemical reactions starting from commercially available building blocks (Auto-Couple) has been developed and successfully applied to the identification of potent and selective bromodomain ligands. This novel approach makes full use of the three-dimensional structure of the protein target and calculates the binding energy by molecular mechanics (transferable force field including electrostatic solvation by the Poisson equation) without any fitting parameter. Thus, AutoCouple is a fragment-growing program that generates synthetically accessible molecules with an accurate and efficient prediction of their binding energy. Our in silico guided medicinal chemistry optimization represents a very efficient strategy to expand the chemical diversity while swiftly acquiring knowledge on previously unexplored areas of chemical space for the target of choice.

AutoCouple has been benchmarked on the CBP bromodomain taking an existing hit as starting point for a ligand optimization campaign. While only potency and synthetic accessibility were encoded in the design working principles of AutoCouple, highly potent and selective ligands with improved solubility and cell permeability have been identified, thus underpinning the importance of chemical diversity in tackling properties that are hard to predict with existing softwares. Hit expansion by AutoCouple resulted in compound **16**, a cell-permeable ligand of the CBP bromodomain with low-nanomolar potency and high selectivity against BRD4(1). This probe represents a useful chemical tool to unravel the individual role of CBP in several types of diseases including cancer, inflammation, and hematological malignancies among others. Further biological evaluation of these compounds and application of AutoCouple to other protein targets are currently ongoing in our laboratories.

ASSOCIATED CONTENT

Ⓢ Supporting Information

The Supporting Information is available free of charge on the ACS Publications website at DOI: 10.1021/acscentsci.7b00401.

> Computational methods, organic syntheses, NMR traces, UV traces, biophysical analyses, and crystallographic data (PDF)

AUTHOR INFORMATION

Corresponding Authors
*E-mail: caflisch@bioc.uzh.ch.
*E-mail: cristina.nevado@chem.uzh.ch.

ORCID Ⓞ
Cristina Nevado: 0000-0002-3297-581X
Amedeo Caflisch: 0000-0002-2317-6792

Author Contributions
[‡]L.B. and A.U. contributed equally to this work.

Notes
The authors declare no competing financial interest.

ABBREVIATIONS

BET, bromo- and extraterminal domain; BRD4(1), first bromodomain of the protein called BRD4; CBP, binding protein of the cyclic AMP response element binding protein; KAc, acetylated lysine; ROC, receiver operating characteristic; FRAP, fluorescence recovery after photobleaching; K_d, dissociation constant; SEED, solvation energy for exhaustive docking; GFP, green fluorescent protein

REFERENCES

(1) Fink, T.; Reymond, J.-L. Virtual Exploration of the Chemical Universe up to 11 Atoms of C, N, O, F: Assembly of 26.4 Million Structures (110.9 Million Stereoisomers) and Analysis for New Ring Systems, Stereochemistry, Physicochemical Properties, Compound Classes, and Drug Discovery. *J. Chem. Inf. Model.* **2007**, *47*, 342−353.

(2) Dragone, V.; Sans, V.; Henson, A. B.; Granda, J. M.; Cronin, L. An autonomous organic reaction search engine for chemical reactivity. *Nat. Commun.* **2017**, 8:15733.

(3) Warne, T.; Serrano-Vega, M. J.; Baker, J. G.; Moukhametzianov, R.; Edwards, P. C.; Henderson, R.; Leslie, A. G. W.; Tate, C. G.; Schertler, G. F. X. Structure of a β1-adrenergic G-protein-coupled receptor. *Nature* **2008**, *454*, 486−491.

(4) Lucas, X.; Grüning, B. A.; Bleher, S.; Günther, S. The Purchasable Chemical Space: A Detailed Picture. *J. Chem. Inf. Model.* **2015**, *55*, 915−924.

(5) Hartenfeller, M.; Eberle, M.; Meier, P.; Nieto-Oberhuber, C.; Altmann, K.-H.; Schneider, G.; Jacoby, E.; Renner, S. Probing the Bioactivity-Relevant Chemical Space of Robust Reactions and Common Molecular Building Blocks. *J. Chem. Inf. Model.* **2012**, *52*, 1167−1178.

(6) Wetzel, S.; Bon, R. S.; Kumar, K.; Waldmann, H. Biology-Oriented Synthesis. *Angew. Chem., Int. Ed.* **2011**, *50*, 10800−10826.

(7) Burke, M. D.; Schreiber, S. L. A Planning Strategy for Diversity-Oriented Synthesis. *Angew. Chem., Int. Ed.* **2004**, *43*, 46−58.

(8) Dandapani, S.; Marcaurelle, L. A. Grand challenge commentary: Accessing new chemical space for 'undruggable' targets. *Nat. Chem. Biol.* **2010**, *6*, 861−863.

(9) Vidler, L. R.; Brown, N.; Knapp, S.; Hoelder, S. Druggability Analysis and Structural Classification of Bromodomain Acetyl-lysine Binding Sites. *J. Med. Chem.* **2012**, *55*, 7346−7359.

(10) Zhang, G.; Sanchez, R.; Zhou, M.-M. Scaling the Druggability Landscape of Human Bromodomains, a New Class of Drug Targets. *J. Med. Chem.* **2012**, *55*, 7342−7345.

(11) Valeur, E.; Guéret, S. M.; Adihou, H.; Gopalakrishnan, R.; Lemurell, M.; Waldmann, H.; Grossmann, T. N.; Plowright, A. T. New Modalities for Challenging Targets in Drug Discovery. *Angew. Chem., Int. Ed.* **2017**, *56*, 10294−10323.

(12) Hartenfeller, M.; Schneider, G. In *Chemoinformatics and Computational Chemical Biology*; Bajorath, J., Ed.; Humana Press: Totowa, NJ, 2011; pp 299−323.

(13) Schneider, G.; Fechner, U. Computer-based de novo design of drug-like molecules. *Nat. Rev. Drug Discovery* 2005, 4, 649−663.

(14) Chéron, N.; Jasty, N.; Shakhnovich, E. I. OpenGrowth: An Automated and Rational Algorithm for Finding New Protein Ligands. *J. Med. Chem.* 2016, 59, 4171−4188.

(15) Yuan, Y.; Pei, J.; Lai, L. LigBuilder 2: A Practical de Novo Drug Design Approach. *J. Chem. Inf. Model.* 2011, 51, 1083−1091.

(16) Wang, R.; Gao, Y.; Lai, L. LigBuilder: A Multi-Purpose Program for Structure-Based Drug Design. *J. Mol. Model.* 2000, 6, 498−516.

(17) Liu, T.; Naderi, M.; Alvin, C.; Mukhopadhyay, S.; Brylinski, M. Break Down in Order To Build Up: Decomposing Small Molecules for Fragment-Based Drug Design with eMolFrag. *J. Chem. Inf. Model.* 2017, 57, 627−631.

(18) Ghersi, D.; Singh, M. molBLOCKS: decomposing small molecule sets and uncovering enriched fragments. *Bioinformatics* 2014, 30, 2081−2083.

(19) Naderi, M.; Alvin, C.; Ding, Y.; Mukhopadhyay, S.; Brylinski, M. A graph-based approach to construct target-focused libraries for virtual screening. *J. Cheminf.* 2016, 8, 14.

(20) Cooper, T. W. J.; Campbell, I. B.; Macdonald, S. J. F. Factors Determining the Selection of Organic Reactions by Medicinal Chemists and the Use of These Reactions in Arrays (Small Focused Libraries). *Angew. Chem., Int. Ed.* 2010, 49, 8082−8091.

(21) Hartenfeller, M.; Zettl, H.; Walter, M.; Rupp, M.; Reisen, F.; Proschak, E.; Weggen, S.; Stark, H.; Schneider, G. DOGS: Reaction-Driven de novo Design of Bioactive Compounds. *PLoS Comput. Biol.* 2012, 8, e1002380.

(22) Chevillard, F.; Kolb, P. SCUBIDOO: A Large yet Screenable and Easily Searchable Database of Computationally Created Chemical Compounds Optimized toward High Likelihood of Synthetic Tractability. *J. Chem. Inf. Model.* 2015, 55, 1824−1835.

(23) Vinkers, H. M.; de Jonge, M. R.; Daeyaert, F. F. D.; Heeres, J.; Koymans, L. M. H.; van Lenthe, J. H.; Lewi, P. J.; Timmerman, H.; Van Aken, K.; Janssen, P. A. J. SYNOPSIS: SYNthesize and OPtimize System in Silico. *J. Med. Chem.* 2003, 46, 2765−2773.

(24) Schneider, G.; Lee, M.-L.; Stahl, M.; Schneider, P. De novo design of molecular architectures by evolutionary assembly of drug-derived building blocks. *J. Comput.-Aided Mol. Des.* 2000, 14, 487−494.

(25) Filippakopoulos, P.; Knapp, S. Targeting bromodomains: epigenetic readers of lysine acetylation. *Nat. Rev. Drug Discovery* 2014, 13, 337−356.

(26) Muller, S.; Filippakopoulos, P.; Knapp, S. Bromodomains as therapeutic targets. *Expert Rev. Mol. Med.* 2011, 13, e29.

(27) Lucas, X.; Wohlwend, D.; Hügle, M.; Schmidtkunz, K.; Gerhardt, S.; Schüle, R.; Jung, M.; Einsle, O.; Günther, S. 4-Acyl Pyrroles: Mimicking Acetylated Lysines in Histone Code Reading. *Angew. Chem., Int. Ed.* 2013, 52, 14055−14059.

(28) Hügle, M.; Lucas, X.; Ostrovskyi, D.; Regenass, P.; Gerhardt, S.; Einsle, O.; Hau, M.; Jung, M.; Breit, B.; Günther, S.; Wohlwend, D. Beyond the BET Family: Targeting CBP/p300 with 4-Acyl Pyrroles. *Angew. Chem., Int. Ed.* 2017, 56, 12476−12480.

(29) Filippakopoulos, P.; Qi, J.; Picaud, S.; Shen, Y.; Smith, W. B.; Fedorov, O.; Morse, E. M.; Keates, T.; Hickman, T. T.; Felletar, I.; Philpott, M.; Munro, S.; McKeown, M. R.; Wang, Y.; Christie, A. L.; West, N.; Cameron, M. J.; Schwartz, B.; Heightman, T. D.; La Thangue, N.; French, C. A.; Wiest, O.; Kung, A. L.; Knapp, S.; Bradner, J. E. Selective inhibition of BET bromodomains. *Nature* 2010, 468, 1067−1073.

(30) Zhao, H.; Gartenmann, L.; Dong, J.; Spiliotopoulos, D.; Caflisch, A. Discovery of BRD4 bromodomain inhibitors by fragment-based high-throughput docking. *Bioorg. Med. Chem. Lett.* 2014, 24, 2493−2496.

(31) Conway, S. J.; Woster, P. M.; Greenlee, W. J.; Georg, G.; Wang, S. Epigenetics: Novel Therapeutics Targeting Epigenetics. *J. Med. Chem.* 2016, 59, 1247−1248.

(32) Andrieu, G.; Belkina, A. C.; Denis, G. V. Clinical trials for BET inhibitors run ahead of the science. *Drug Discovery Today: Technol.* 2016, 19, 45−50.

(33) Wadhwa, E.; Nicolaides, T. Bromodomain Inhibitor Review: Bromodomain and Extra-terminal Family Protein Inhibitors as a Potential New Therapy in Central Nervous System Tumors. *Cureus* 2016, 8, e620.

(34) Zhang, G.; Smith, S. G.; Zhou, M.-M. Discovery of Chemical Inhibitors of Human Bromodomains. *Chem. Rev.* 2015, 115, 11625−11668.

(35) Romero, F. A.; Taylor, A. M.; Crawford, T. D.; Tsui, V.; Côté, A.; Magnuson, S. Disrupting Acetyl-Lysine Recognition: Progress in the Development of Bromodomain Inhibitors. *J. Med. Chem.* 2016, 59, 1271−1298.

(36) Hewings, D. S.; Rooney, T. P. C.; Jennings, L. E.; Hay, D. A.; Schofield, C. J.; Brennan, P. E.; Knapp, S.; Conway, S. J. Progress in the Development and Application of Small Molecule Inhibitors of Bromodomain−Acetyl-lysine Interactions. *J. Med. Chem.* 2012, 55, 9393−9413.

(37) Gallenkamp, D.; Gelato, K. A.; Haendler, B.; Weinmann, H. Bromodomains and Their Pharmacological Inhibitors. *ChemMedChem* 2014, 9, 438−464.

(38) Berthon, C.; Raffoux, E.; Thomas, X.; Vey, N.; Gomez-Roca, C.; Yee, K.; Taussig, D. C.; Rezai, K.; Roumier, C.; Herait, P.; Kahatt, C.; Quesnel, B.; Michallet, M.; Recher, C.; Lokiec, F.; Preudhomme, C.; Dombret, H. Bromodomain inhibitor OTX015 in patients with acute leukaemia: a dose-escalation, phase 1 study. *Lancet Haematology* 2016, 3, e186−e195.

(39) Clark, P. G. K.; Vieira, L. C. C.; Tallant, C.; Fedorov, O.; Singleton, D. C.; Rogers, C. M.; Monteiro, O. P.; Bennett, J. M.; Baronio, R.; Müller, S.; Daniels, D. L.; Méndez, J.; Knapp, S.; Brennan, P. E.; Dixon, D. J. LP99: Discovery and Synthesis of the First Selective BRD7/9 Bromodomain Inhibitor. *Angew. Chem., Int. Ed.* 2015, 54, 6217−6221.

(40) Bamborough, P.; Chung, C.-w.; Furze, R. C.; Grandi, P.; Michon, A.-M.; Sheppard, R. J.; Barnett, H.; Diallo, H.; Dixon, D. P.; Douault, C.; Jones, E. J.; Karamshi, B.; Mitchell, D. J.; Prinjha, R. K.; Rau, C.; Watson, R. J.; Werner, T.; Demont, E. H. Structure-Based Optimization of Naphthyridones into Potent ATAD2 Bromodomain Inhibitors. *J. Med. Chem.* 2015, 58, 6151−6178.

(41) Hay, D. A.; Rogers, C. M.; Fedorov, O.; Tallant, C.; Martin, S.; Monteiro, O. P.; Müller, S.; Knapp, S.; Schofield, C. J.; Brennan, P. E. Design and synthesis of potent and selective inhibitors of BRD7 and BRD9 bromodomains. *MedChemComm* 2015, 6, 1381−1386.

(42) Lolli, G.; Caflisch, A. High-Throughput Fragment Docking into the BAZ2B Bromodomain: Efficient in Silico Screening for X-Ray Crystallography. *ACS Chem. Biol.* 2016, 11, 800−807.

(43) Theodoulou, N. H.; Bamborough, P.; Bannister, A. J.; Becher, I.; Bit, R. A.; Che, K. H.; Chung, C.-w.; Dittmann, A.; Drewes, G.; Drewry, D. H.; Gordon, L.; Grandi, P.; Leveridge, M.; Lindon, M.; Michon, A.-M.; Molnar, J.; Robson, S. C.; Tomkinson, N. C. O.; Kouzarides, T.; Prinjha, R. K.; Humphreys, P. G. Discovery of I-BRD9, a Selective Cell Active Chemical Probe for Bromodomain Containing Protein 9 Inhibition. *J. Med. Chem.* 2016, 59, 1425−1439.

(44) Zucconi, B. E.; Luef, B.; Xu, W.; Henry, R. A.; Nodelman, I. M.; Bowman, G. D.; Andrews, A. J.; Cole, P. A. Modulation of p300/CBP Acetylation of Nucleosomes by Bromodomain Ligand I-CBP112. *Biochemistry* 2016, 55, 3727−3734.

(45) Navratilova, I.; Aristotelous, T.; Picaud, S.; Chaikuad, A.; Knapp, S.; Filappakopoulos, P.; Hopkins, A. L. Discovery of New Bromodomain Scaffolds by Biosensor Fragment Screening. *ACS Med. Chem. Lett.* 2016, 7, 1213−1218.

(46) Palmer, W. S. Development of small molecule inhibitors of BRPF1 and TRIM24 bromodomains. *Drug Discovery Today: Technol.* 2016, 19, 65−71.

(47) Palmer, W. S.; Poncet-Montange, G.; Liu, G.; Petrocchi, A.; Reyna, N.; Subramanian, G.; Theroff, J.; Yau, A.; Kost-Alimova, M.; Bardenhagen, J. P.; Leo, E.; Shepard, H. E.; Tieu, T. N.; Shi, X.; Zhan, Y.; Zhao, S.; Barton, M. C.; Draetta, G.; Toniatti, C.; Jones, P.; Geck

Do, M.; Andersen, J. N. Structure-Guided Design of IACS-9571, a Selective High-Affinity Dual TRIM24-BRPF1 Bromodomain Inhibitor. *J. Med. Chem.* **2016**, *59*, 1440−1454.

(48) Bamborough, P.; Barnett, H. A.; Becher, I.; Bird, M. J.; Chung, C.-w.; Craggs, P. D.; Demont, E. H.; Diallo, H.; Fallon, D. J.; Gordon, L. J.; Grandi, P.; Hobbs, C. I.; Hooper-Greenhill, E.; Jones, E. J.; Law, R. P.; Le Gall, A.; Lugo, D.; Michon, A.-M.; Mitchell, D. J.; Prinjha, R. K.; Sheppard, R. J.; Watson, A. J. B.; Watson, R. J. GSK6853, a Chemical Probe for Inhibition of the BRPF1 Bromodomain. *ACS Med. Chem. Lett.* **2016**, *7*, 552−557.

(49) Zhu, J.; Caflisch, A. Twenty Crystal Structures of Bromodomain and PHD Finger Containing Protein 1 (BRPF1)/Ligand Complexes Reveal Conserved Binding Motifs and Rare Interactions. *J. Med. Chem.* **2016**, *59*, 5555−5561.

(50) Demont, E. H.; Bamborough, P.; Chung, C.-w.; Craggs, P. D.; Fallon, D.; Gordon, L. J.; Grandi, P.; Hobbs, C. I.; Hussain, J.; Jones, E. J.; Le Gall, A.; Michon, A.-M.; Mitchell, D. J.; Prinjha, R. K.; Roberts, A. D.; Sheppard, R. J.; Watson, R. J. 1,3-Dimethyl Benzimidazolones Are Potent, Selective Inhibitors of the BRPF1 Bromodomain. *ACS Med. Chem. Lett.* **2014**, *5*, 1190−1195.

(51) Bennett, J.; Fedorov, O.; Tallant, C.; Monteiro, O.; Meier, J.; Gamble, V.; Savitsky, P.; Nunez-Alonso, G. A.; Haendler, B.; Rogers, C.; Brennan, P. E.; Müller, S.; Knapp, S. Discovery of a Chemical Tool Inhibitor Targeting the Bromodomains of TRIM24 and BRPF. *J. Med. Chem.* **2016**, *59*, 1642−1647.

(52) Demont, E. H.; Chung, C.-w.; Furze, R. C.; Grandi, P.; Michon, A.-M.; Wellaway, C.; Barrett, N.; Bridges, A. M.; Craggs, P. D.; Diallo, H.; Dixon, D. P.; Douault, C.; Emmons, A. J.; Jones, E. J.; Karamshi, B. V.; Locke, K.; Mitchell, D. J.; Mouzon, B. H.; Prinjha, R. K.; Roberts, A. D.; Sheppard, R. J.; Watson, R. J.; Bamborough, P. Fragment-Based Discovery of Low-Micromolar ATAD2 Bromodomain Inhibitors. *J. Med. Chem.* **2015**, *58*, 5649−5673.

(53) Bamborough, P.; Chung, C.-w.; Demont, E. H.; Furze, R. C.; Bannister, A. J.; Che, K. H.; Diallo, H.; Douault, C.; Grandi, P.; Kouzarides, T.; Michon, A.-M.; Mitchell, D. J.; Prinjha, R. K.; Rau, C.; Robson, S.; Sheppard, R. J.; Upton, R.; Watson, R. J. A Chemical Probe for the ATAD2 Bromodomain. *Angew. Chem., Int. Ed.* **2016**, *55*, 11382−11386.

(54) Moustakim, M.; Clark, P. G. K.; Trulli, L.; Fuentes de Arriba, A. L.; Ehebauer, M. T.; Chaikuad, A.; Murphy, E. J.; Mendez-Johnson, J.; Daniels, D.; Hou, C.-F. D.; Lin, Y.-H.; Walker, J. R.; Hui, R.; Yang, H.; Dorrell, L.; Rogers, C. M.; Monteiro, O. P.; Fedorov, O.; Huber, K. V. M; Knapp, S.; Heer, J.; Dixon, D. J.; Brennan, P. E. Discovery of a PCAF Bromodomain Chemical Probe. *Angew. Chem., Int. Ed.* **2017**, *56*, 827−831.

(55) Theodoulou, N. H.; Tomkinson, N. C. O.; Prinjha, R. K.; Humphreys, P. G. Progress in the Development of non-BET Bromodomain Chemical Probes. *ChemMedChem* **2016**, *11*, 477−487.

(56) Rooney, T. P. C.; Filippakopoulos, P.; Fedorov, O.; Picaud, S.; Cortopassi, W. A.; Hay, D. A.; Martin, S.; Tumber, A.; Rogers, C. M.; Philpott, M.; Wang, M.; Thompson, A. L.; Heightman, T. D.; Pryde, D. C.; Cook, A.; Paton, R. S.; Müller, S.; Knapp, S.; Brennan, P. E.; Conway, S. J. A Series of Potent CREBBP Bromodomain Ligands Reveals an Induced-Fit Pocket Stabilized by a Cation−π Interaction. *Angew. Chem., Int. Ed.* **2014**, *53*, 6126−6130.

(57) Hammitzsch, A.; Tallant, C.; Fedorov, O.; O'Mahony, A.; Brennan, P. E.; Hay, D. A.; Martinez, F. O.; Al-Mossawi, M. H.; de Wit, J.; Vecellio, M.; Wells, C.; Wordsworth, P.; Müller, S.; Knapp, S.; Bowness, P. CBP30, a selective CBP/p300 bromodomain inhibitor, suppresses human Th17 responses. *Proc. Natl. Acad. Sci. U. S. A.* **2015**, *112*, 10768−10773.

(58) Taylor, A. M.; Côté, A.; Hewitt, M. C.; Pastor, R.; Leblanc, Y.; Nasveschuk, C. G.; Romero, F. A.; Crawford, T. D.; Cantone, N.; Jayaram, H.; Setser, J.; Murray, J.; Beresini, M. H.; de Leon Boenig, G.; Chen, Z.; Conery, A. R.; Cummings, R. T.; Dakin, L. A.; Flynn, E. M.; Huang, O. W.; Kaufman, S.; Keller, P. J.; Kiefer, J. R.; Lai, T.; Li, Y.; Liao, J.; Liu, W.; Lu, H.; Pardo, E.; Tsui, V.; Wang, J.; Wang, Y.; Xu, Z.; Yan, F.; Yu, D.; Zawadzke, L.; Zhu, X.; Zhu, X.; Sims, R. J.; Cochran, A. G.; Bellon, S.; Audia, J. E.; Magnuson, S.; Albrecht, B. K. Fragment-Based Discovery of a Selective and Cell-Active Benzodiazepinone CBP/EP300 Bromodomain Inhibitor (CPI-637). *ACS Med. Chem. Lett.* **2016**, *7*, 531−536.

(59) Crawford, T. D.; Romero, F. A.; Lai, K. W.; Tsui, V.; Taylor, A. M.; de Leon Boenig, G.; Noland, C. L.; Murray, J.; Ly, J.; Choo, E. F.; Hunsaker, T. L.; Chan, E. W.; Merchant, M.; Kharbanda, S.; Gascoigne, K. E.; Kaufman, S.; Beresini, M. H.; Liao, J.; Liu, W.; Chen, K. X.; Chen, Z.; Conery, A. R.; Côté, A.; Jayaram, H.; Jiang, Y.; Kiefer, J. R.; Kleinheinz, T.; Li, Y.; Maher, J.; Pardo, E.; Poy, F.; Spillane, K. L.; Wang, F.; Wang, J.; Wei, X.; Xu, Z.; Xu, Z.; Yen, I.; Zawadzke, L.; Zhu, X.; Bellon, S.; Cummings, R.; Cochran, A. G.; Albrecht, B. K.; Magnuson, S. Discovery of a Potent and Selective in Vivo Probe (GNE-272) for the Bromodomains of CBP/EP300. *J. Med. Chem.* **2016**, *59*, 10549−10563.

(60) Romero, F. A.; Murray, J.; Lai, K. W.; Tsui, V.; Albrecht, B. K.; An, L.; Beresini, M. H.; de Leon Boenig, G.; Bronner, S. M.; Chan, E. W.; Chen, K. X.; Chen, Z.; Choo, E. F.; Clagg, K.; Clark, K.; Crawford, T. D.; Cyr, P.; de Almeida Nagata, D.; Gascoigne, K. E.; Grogan, J. L.; Hatzivassiliou, G.; Huang, W.; Hunsaker, T. L.; Kaufman, S.; Koenig, S. G.; Li, R.; Li, Y.; Liang, X.; Liao, J.; Liu, W.; Ly, J.; Maher, J.; Masui, C.; Merchant, M.; Ran, Y.; Taylor, A. M.; Wai, J.; Wang, F.; Wei, X.; Yu, D.; Zhu, B.-Y.; Zhu, X.; Magnuson, S. GNE-781, A Highly Advanced Potent and Selective Bromodomain Inhibitor of Cyclic Adenosine Monophosphate Response Element Binding Protein, Binding Protein (CBP). *J. Med. Chem.* **2017**, *60*, 9162.

(61) Hay, D. A.; Fedorov, O.; Martin, S.; Singleton, D. C.; Tallant, C.; Wells, C.; Picaud, S.; Philpott, M.; Monteiro, O. P.; Rogers, C. M.; Conway, S. J.; Rooney, T. P. C.; Tumber, A.; Yapp, C.; Filippakopoulos, P.; Bunnage, M. E.; Müller, S.; Knapp, S.; Schofield, C. J.; Brennan, P. E. Discovery and Optimization of Small-Molecule Ligands for the CBP/p300 Bromodomains. *J. Am. Chem. Soc.* **2014**, *136*, 9308−9319.

(62) Picaud, S.; Fedorov, O.; Thanasopoulou, A.; Leonards, K.; Jones, K.; Meier, J.; Olzscha, H.; Monteiro, O.; Martin, S.; Philpott, M.; Tumber, A.; Filippakopoulos, P.; Yapp, C.; Wells, C.; Che, K. H.; Bannister, A.; Robson, S.; Kumar, U.; Parr, N.; Lee, K.; Lugo, D.; Jeffrey, P.; Taylor, S.; Vecellio, M. L.; Bountra, C.; Brennan, P. E.; O'Mahony, A.; Velichko, S.; Müller, S.; Hay, D.; Daniels, D. L.; Urh, M.; La Thangue, N. B.; Kouzarides, T.; Prinjha, R.; Schwaller, J.; Knapp, S. Generation of a Selective Small Molecule Inhibitor of the CBP/p300 Bromodomain for Leukemia Therapy. *Cancer Res.* **2015**, *75*, 5106−5119.

(63) Denny, R. A.; Flick, A. C.; Coe, J.; Langille, J.; Basak, A.; Liu, S.; Stock, I.; Sahasrabudhe, P.; Bonin, P.; Hay, D. A.; Brennan, P. E.; Pletcher, M.; Jones, L. H.; Chekler, E. L. P. Structure-Based Design of Highly Selective Inhibitors of the CREB Binding Protein Bromodomain. *J. Med. Chem.* **2017**, *60*, 5349−5363.

(64) Popp, T. A.; Tallant, C.; Rogers, C.; Fedorov, O.; Brennan, P. E.; Müller, S.; Knapp, S.; Bracher, F. Development of Selective CBP/P300 Benzoxazepine Bromodomain Inhibitors. *J. Med. Chem.* **2016**, *59*, 8889−8912.

(65) Moustakim, M.; Clark, P. G.; Hay, D. A.; Dixon, D. J.; Brennan, P. E. Chemical probes and inhibitors of bromodomains outside the BET family. *MedChemComm* **2016**, *7*, 2246−2264.

(66) Ghosh, S.; Taylor, A.; Chin, M.; Huang, H.-R.; Conery, A. R.; Mertz, J. A.; Salmeron, A.; Dakle, P. J.; Mele, D.; Cote, A.; et al. Regulatory T cell modulation by CBP/EP300 bromodomain inhibition. *J. Biol. Chem.* **2016**, *291*, 13014−13027.

(67) Gerona-Navarro, G.; Yoel-Rodríguez; Mujtaba, S.; Frasca, A.; Patel, J.; Zeng, L.; Plotnikov, A. N.; Osman, R.; Zhou, M.-M. Rational Design of Cyclic Peptide Modulators of the Transcriptional Coactivator CBP: A New Class of p53 Inhibitors. *J. Am. Chem. Soc.* **2011**, *133*, 2040−2043.

(68) Majeux, N.; Scarsi, M.; Apostolakis, J.; Ehrhardt, C.; Caflisch, A. Exhaustive docking of molecular fragments with electrostatic solvation. *Proteins: Struct., Funct., Genet.* **1999**, *37*, 88−105.

(69) Majeux, N.; Scarsi, M.; Caflisch, A. Efficient electrostatic solvation model for protein-fragment docking. *Proteins: Struct., Funct., Genet.* **2001**, *42*, 256−268.

(70) Xu, M.; Unzue, A.; Dong, J.; Spiliotopoulos, D.; Nevado, C.; Caflisch, A. Discovery of CREBBP Bromodomain Inhibitors by High-Throughput Docking and Hit Optimization Guided by Molecular Dynamics. *J. Med. Chem.* **2016**, *59*, 1340−1349.

(71) Unzue, A.; Xu, M.; Dong, J.; Wiedmer, L.; Spiliotopoulos, D.; Caflisch, A.; Nevado, C. Fragment-Based Design of Selective Nanomolar Ligands of the CREBBP Bromodomain. *J. Med. Chem.* **2016**, *59*, 1350−1356.

(72) Paul, S. M.; Mytelka, D. S.; Dunwiddie, C. T.; Persinger, C. C.; Munos, B. H.; Lindborg, S. R.; Schacht, A. L. How to improve R&D productivity: the pharmaceutical industry's grand challenge. *Nat. Rev. Drug Discovery* **2010**, *9*, 203−214.

(73) Kubinyi, H. Drug research: myths, hype and reality. *Nat. Rev. Drug Discovery* **2003**, *2*, 665−668.

(74) Kola, I.; Landis, J. Can the pharmaceutical industry reduce attrition rates? *Nat. Rev. Drug Discovery* **2004**, *3*, 711−716.

(75) Coley, C. W.; Barzilay, R.; Jaakkola, T. S.; Green, W. H.; Jensen, K. F. Prediction of Organic Reaction Outcomes Using Machine Learning. *ACS Cent. Sci.* **2017**, *3*, 434−443.

(76) Kayala, M. A.; Baldi, P. ReactionPredictor: Prediction of Complex Chemical Reactions at the Mechanistic Level Using Machine Learning. *J. Chem. Inf. Model.* **2012**, *52*, 2526−2540.

(77) Dutta, R.; Tiu, B.; Sakamoto, K. M. CBP/p300 acetyltransferase activity in hematologic malignancies. *Mol. Genet. Metab.* **2016**, *119*, 37−43.

(78) VanRossum, G.; Drake, F. L.; *The Python Language Reference*; Python software foundation: Amsterdam, Netherlands, 2010.

(79) Landrum, G.; RDKit, Open-Source Cheminformatics; *Online:* http://www.rdkit.org.

(80) Hartenfeller, M.; Eberle, M.; Meier, P.; Nieto-Oberhuber, C.; Altmann, K.-H.; Schneider, G.; Jacoby, E.; Renner, S. A Collection of Robust Organic Synthesis Reactions for In Silico Molecule Design. *J. Chem. Inf. Model.* **2011**, *51*, 3093−3098.

(81) Rishton, G. M. Reactive compounds and in vitro false positives in HTS. *Drug Discovery Today* **1997**, *2*, 382−384.

(82) Baell, J. B.; Holloway, G. A. New Substructure Filters for Removal of Pan Assay Interference Compounds (PAINS) from Screening Libraries and for Their Exclusion in Bioassays. *J. Med. Chem.* **2010**, *53*, 2719−2740.

(83) Ruiz-Carmona, S.; Alvarez-Garcia, D.; Foloppe, N.; Garmendia-Doval, A. B.; Juhos, S.; Schmidtke, P.; Barril, X.; Hubbard, R. E.; Morley, S. D. rDock: A Fast, Versatile and Open Source Program for Docking Ligands to Proteins and Nucleic Acids. *PLoS Comput. Biol.* **2014**, *10*, e1003571.

(84) Brooks, B. R.; Brooks, C. L.; Mackerell, A. D.; Nilsson, L.; Petrella, R. J.; Roux, B.; Won, Y.; Archontis, G.; Bartels, C.; Boresch, S.; Caflisch, A.; Caves, L.; Cui, Q.; Dinner, A. R.; Feig, M.; Fischer, S.; Gao, J.; Hodoscek, M.; Im, W.; Kuczera, K.; Lazaridis, T.; Ma, J.; Ovchinnikov, V.; Paci, E.; Pastor, R. W.; Post, C. B.; Pu, J. Z.; Schaefer, M.; Tidor, B.; Venable, R. M.; Woodcock, H. L.; Wu, X.; Yang, W.; York, D. M.; Karplus, M. CHARMM: The biomolecular simulation program. *J. Comput. Chem.* **2009**, *30*, 1545−1614.

(85) Vanommeslaeghe, K.; Hatcher, E.; Acharya, C.; Kundu, S.; Zhong, S.; Shim, J.; Darian, E.; Guvench, O.; Lopes, P.; Vorobyov, I.; Mackerell, A. D. CHARMM general force field: A force field for drug-like molecules compatible with the CHARMM all-atom additive biological force fields. *J. Comput. Chem.* **2010**, *31*, 671−690.

(86) MacKerell, A. D.; Feig, M.; Brooks, C. L. Improved Treatment of the Protein Backbone in Empirical Force Fields. *J. Am. Chem. Soc.* **2004**, *126*, 698−699.

(87) Im, W.; Beglov, D.; Roux, B. Continuum solvation model: Computation of electrostatic forces from numerical solutions to the Poisson-Boltzmann equation. *Comput. Phys. Commun.* **1998**, *111*, 59−75.

(88) Quinn, E.; Wodicka, L.; Ciceri, P.; Pallares, G.; Pickle, E.; Torrey, A.; Floyd, M.; Hunt, J.; Treiber, D. Abstract 4238: BROMOscan - a high throughput, quantitative ligand binding platform identifies best-in-class bromodomain inhibitors from a screen of mature compounds targeting other protein classes. *Cancer Res.* **2013**, *73*, 4238−4238.

(89) Spiliotopoulos, D.; Caflisch, A. Molecular Dynamics Simulations of Bromodomains Reveal Binding-Site Flexibility and Multiple Binding Modes of the Natural Ligand Acetyl-Lysine. *Isr. J. Chem.* **2014**, *54*, 1084−1092.

(90) Unzue, A.; Zhao, H.; Lolli, G.; Dong, J.; Zhu, J.; Zechner, M.; Dolbois, A.; Caflisch, A.; Nevado, C. The "Gatekeeper" Residue Influences the Mode of Binding of Acetyl Indoles to Bromodomains. *J. Med. Chem.* **2016**, *59*, 3087−3097.

(91) Hopkins, A. L.; Keserü, G. M.; Leeson, P. D.; Rees, D. C.; Reynolds, C. H. The role of ligand efficiency metrics in drug discovery. *Nat. Rev. Drug Discovery* **2014**, *13*, 105−121.

(92) Hopkins, A. L.; Groom, C. R.; Alex, A. Ligand efficiency: a useful metric for lead selection. *Drug Discovery Today* **2004**, *9*, 430−431.

(93) For a recent report on a high affinity binder of the bromodomains BRD9, TAF1(2) and of CBP see: Sdelci, S.; Lardeau, C.-H.; Tallant, C.; Klepsch, F.; Klaiber, B.; Bennett, J.; Rathert, P.; Schuster, M.; Penz, T.; Fedorov, O.; Superti-Furga, G.; Bock, C.; Zuber, J.; Huber, K. V. M.; Knapp, S.; Müller, S.; Kubicek, S. Mapping the chemical chromatin reactivation landscape identifies BRD4-TAF1 cross-talk. *Nat. Chem. Biol.* **2016**, *12*, 504−510.

(94) Philpott, M.; Rogers, C. M.; Yapp, C.; Wells, C.; Lambert, J.-P.; Strain-Damerell, C.; Burgess-Brown, N. A.; Gingras, A.-C.; Knapp, S.; Müller, S. Assessing cellular efficacy of bromodomain inhibitors using fluorescence recovery after photobleaching. *Epigenet. Chromatin* **2014**, *7*, 14.

(95) Conery, A. R.; Centore, R. C.; Neiss, A.; Keller, P. J.; Joshi, S.; Spillane, K. L.; Sandy, P.; Hatton, C.; Pardo, E.; Zawadzke, L.; et al. Bromodomain inhibition of the transcriptional coactivators CBP/EP300 as a therapeutic strategy to target the IRF4 network in multiple myeloma. *eLife* **2016**, *5*, e10483.

(96) Jacobs, J.; Jones, C.; Baille, J. Characteristics of a human diploid cell designated MRC-5. *Nature* **1970**, *227*, 168−170.

(97) Hutter, E.; Renner, K.; Pfister, G.; Stöckl, P.; Jansen-Dürr, P.; Gnaiger, E. Senescence-associated changes in respiration and oxidative phosphorylation in primary human fibroblasts. *Biochem. J.* **2004**, *380*, 919−928.

(98) Anoopkumar-Dukie, S.; Carey, J. B.; Conere, T.; O'Sullivan, E.; Pelt, F. N. v.; Allshire, A. Resazurin assay of radiation response in cultured cells. *Br. J. Radiol.* **2005**, *78*, 945−947.

(99) Mertz, J. A.; Conery, A. R.; Bryant, B. M.; Sandy, P.; Balasubramanian, S.; Mele, D. A.; Bergeron, L.; Sims, R. J. Targeting MYC dependence in cancer by inhibiting BET bromodomains. *Proc. Natl. Acad. Sci. U. S. A.* **2011**, *108*, 16669−16674.